
Scattering Wings of the Chandra PSF

Terry Gaetz
SAO



Chandra Calibration Workshop

6 November 2002

- What are the PSF wings?
 - The Her X-1 observation
 - Strut shadows
 - Pileup in the core
 - Data analysis & reduction
 - Wing profiles
 - Summary & Future work
-

The HRMA PSF

The HRMA point spread function (PSF) includes contributions ranging from nearly specular reflection from low frequency figure errors (the “core” of the PSF) to scattered photons reflecting/diffracting off surface microroughness on the optics. The scattered rays form a faint diffuse mirror scattering halo extending to large angles. On-axis, the azimuthally-averaged scattering halo is energy dependent, and approximately powerlaw ($\theta^{-\gamma}$) with $\gamma \sim 2$.

Detailed knowledge of this scattering halo as a function of energy and radius is needed for interpretation of observations with faint structure adjacent to bright sources. Examples might include:

- X-ray scattering halos from cosmic dust along the line of sight
- extracting faint sources adjacent to bright sources
- faint structure (e.g., cosmic ray precursors) ahead of shocks in supernova remnants

Her X-1 Observation (obsid 3662)

In order to refine the calibration of the PSF wings, an observation of an X-ray bright source with low extinction (in order to reduce complications from any cosmic dust scattering halo).

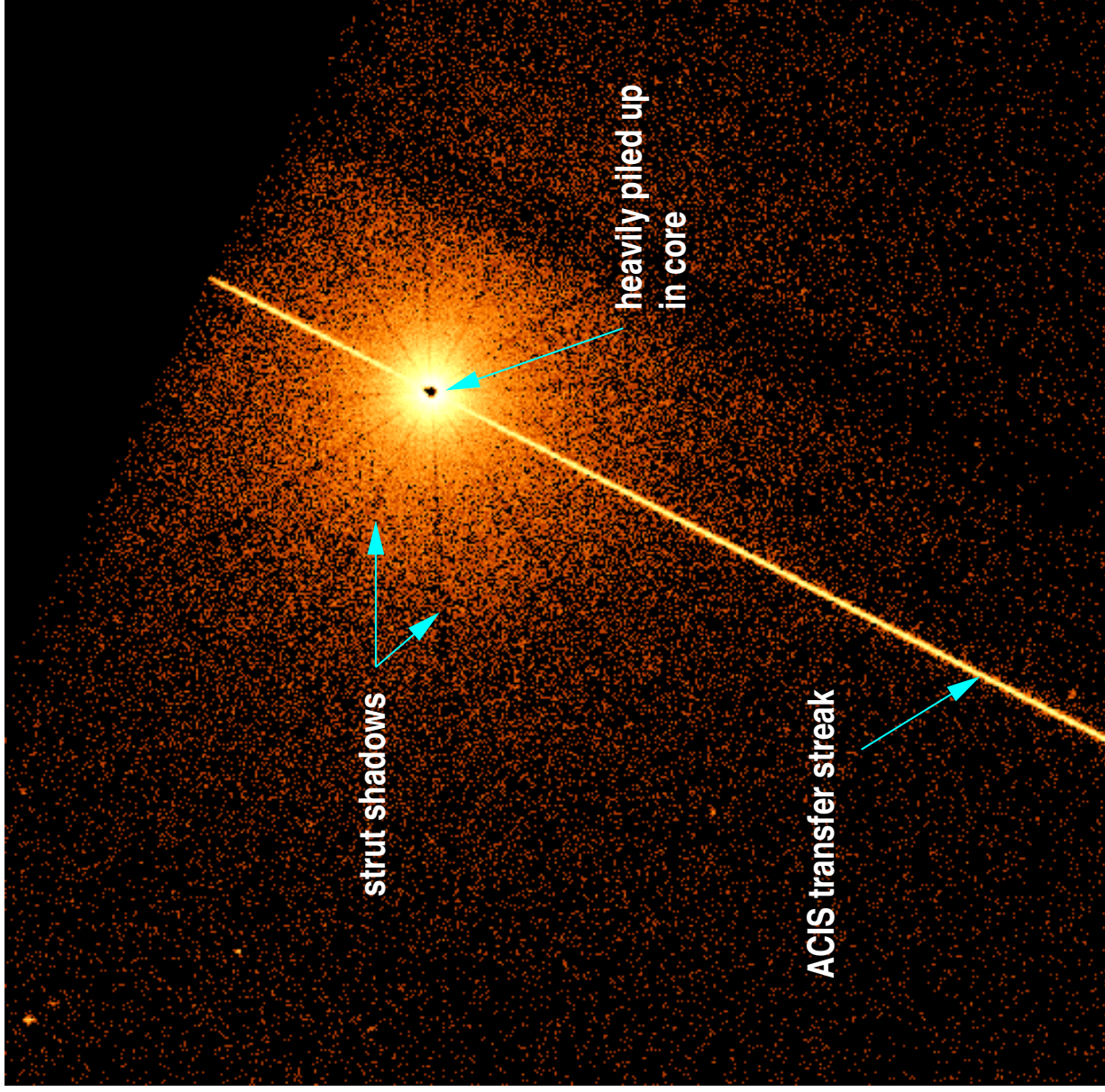
Her X-1 was selected as the target:

- very bright source (allowing wings to be seen against background to large radii, even for narrow energy bins)
- relatively high galactic latitude ($b = 37.52$)
- $E[B - V] \sim 0.05$ (Liu *et al.* 2001)
- Total galactic $N_{\text{H}} \sim 1.8 \times 10^{20} \text{ cm}^{-2}$ (Dickey & Lockman 1991)
- total X-ray cosmic dust scattering halo likely $\lesssim 1.5\%$ (Smith *et al.* 2002)

The observation:

- 50 ks exposure; radiation environment quiescent (no flares)
- Her X-1 was imaged in a corner of the S3 chip, $\sim 45''$ off-axis; this allowed coverage to large off-axis angles on S3, and some exposure of the wings on the FI chips S2, I2, and I3
- VF mode was used; this will allow VF filtering of the data sets

Her X-1 Observation: schematic



Strut Shadows

The lines crossing the image at $\sim 30^\circ$ intervals are shadows cast by the mirror support struts.

Implications:

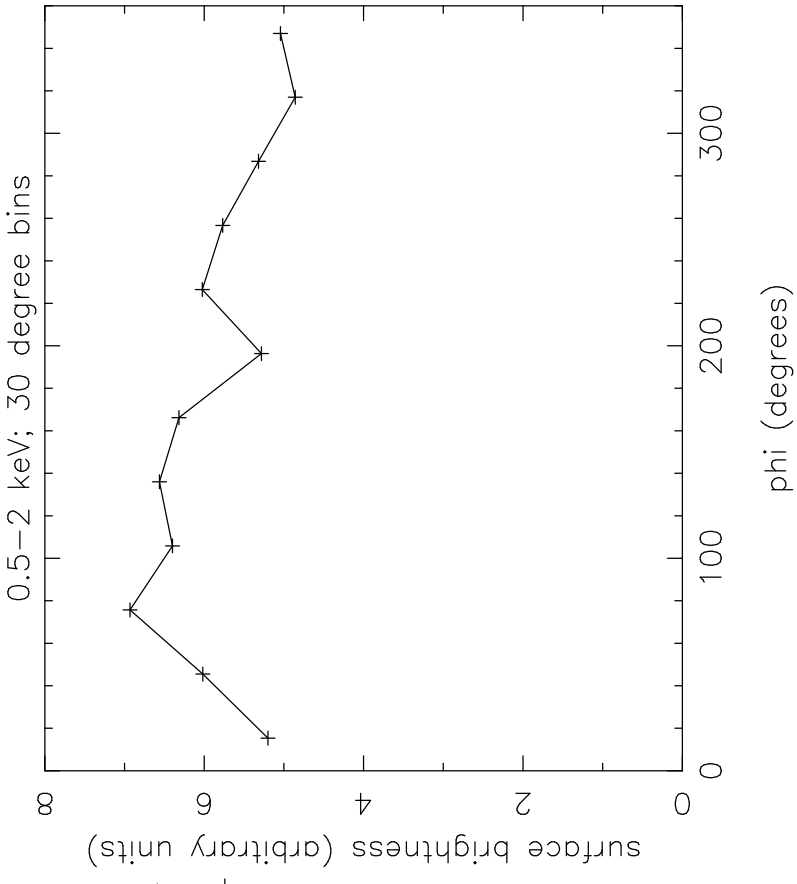
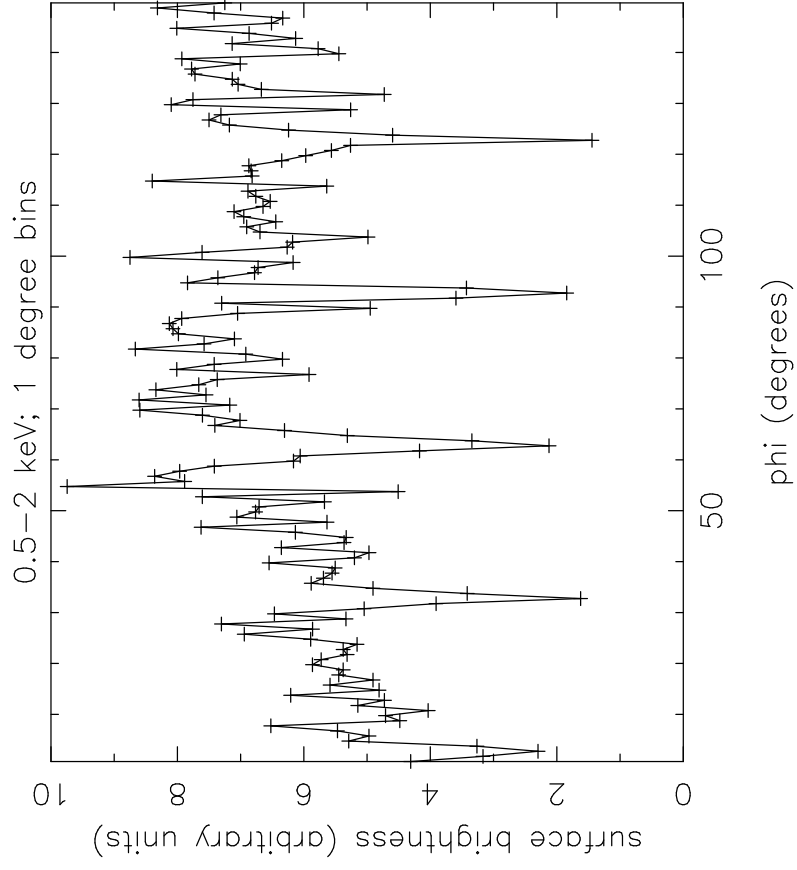
- the halo is predominantly caused by mirror scattering (in-plane) rather than a diffuse astrophysical halo due to dust scattering along the line of sight
- the strut shadows are down in surface brightness by a factor of ≈ 4 .
This gives a strict limit on any contribution from a cosmic dust scattering halo

Analysis complications:

- narrowness of the shadows compared to detector resolution (particularly close in)
- transverse mirror scattering can partially fill in the shadows (needs to be modeled).

Angular distribution

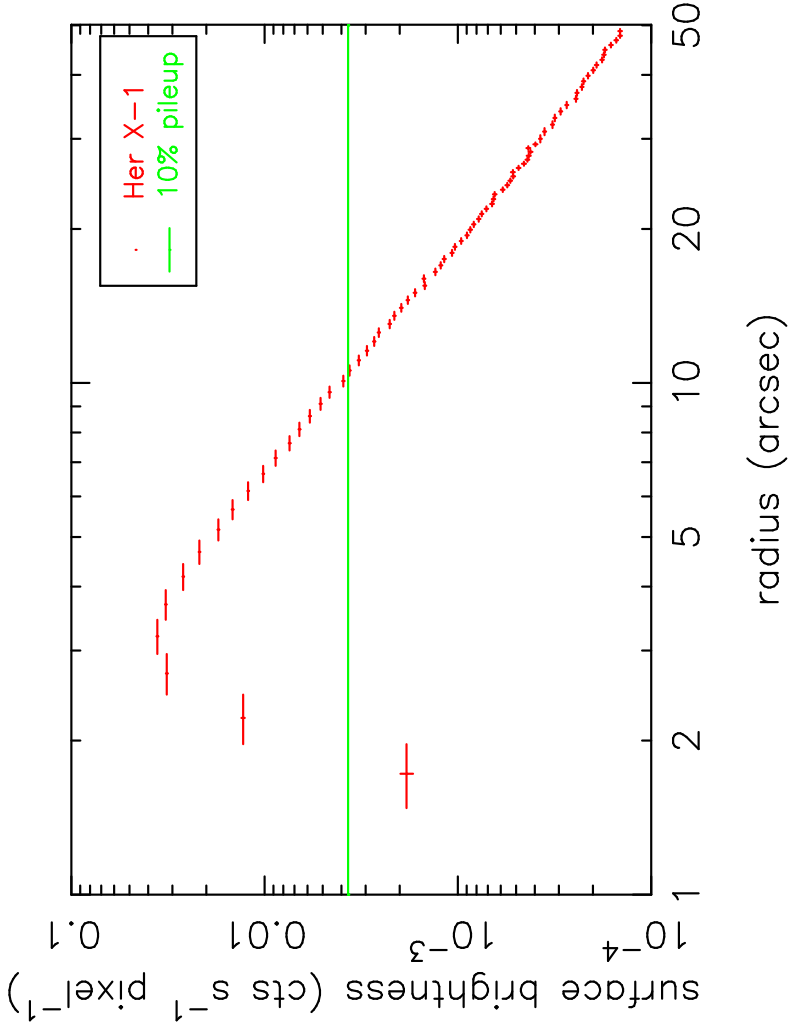
The Her X-1 data will also allow the angular distribution of the mirror scattering to be explored; work on this is underway.



Pileup

The core and inner scattering halo are heavily piled up. The degree of pileup is difficult to assess a priori; it is estimated two ways (following the approach of Smith *et al.* [2002]).

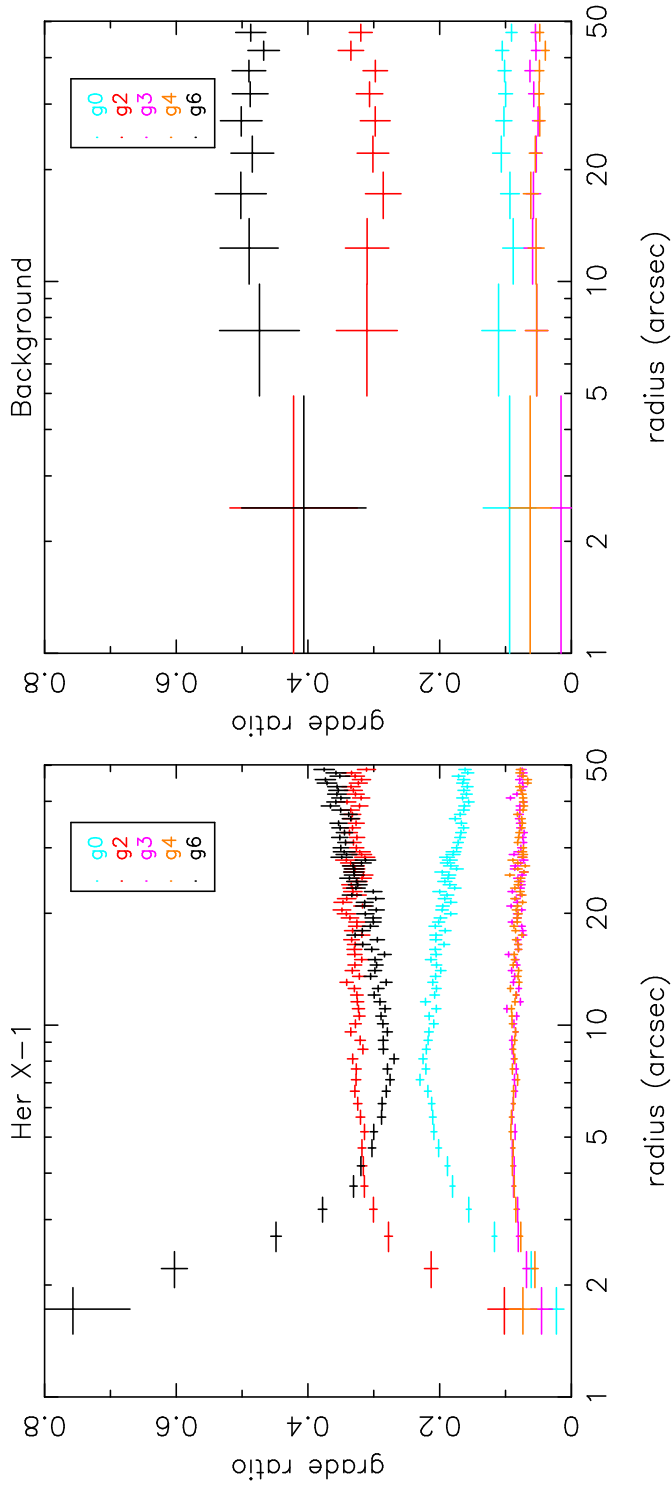
The first approach utilizes surface brightness. For a fairly uniform distribution, Smith *et al.* estimate 10% pileup for a surface brightness $\sim 0.0037 \text{ cts s}^{-1} \text{ pixel}^{-1}$. For the observed Her X-1 surface brightness profile, this indicates $\sim 10\%$ pileup for $\theta \lesssim 10''$.



Grade Ratios and Pileup

Pileup causes [grade migration](#), e.g., converting grade 0 events into grade 6 events.

- Ratios of individual grades to the sum of grades 02346 \rightarrow pileup inside $\sim 5 - 10''$.
- upward trend in grade 6 (and downward trend in grade 0) result from increasing background contribution with radius.



Data Reduction

Initial analysis: S3 data; no VF filtering

- construct narrow-band count images; $\Delta E = 100$ eV to 200 eV; assume a constant spectrum across the band.
- construct dithered QE maps (mkinstmap, mkexppmap)
- QE-corrected image: divide the counts image by the dithered QE image. (Use counts images for error propagation.)
- **Note:** **mirror vignetting function was *not* applied.** The HRMA normalized off-axis effective area (“vignetting function”) is appropriate to **point sources at given off-axis angles**. Scattered photons do not follow the same path through the system; applying the vignetting correction is inappropriate. Scattered photons is included implicitly in calculating the vignetting function.

Background was evaluated from Period D blank sky background files. Narrow-band counts and QE-corrected counts images were constructed in the same manner as for the Her X-1 data.

Data Analysis

Used functions to evaluate radial profiles.

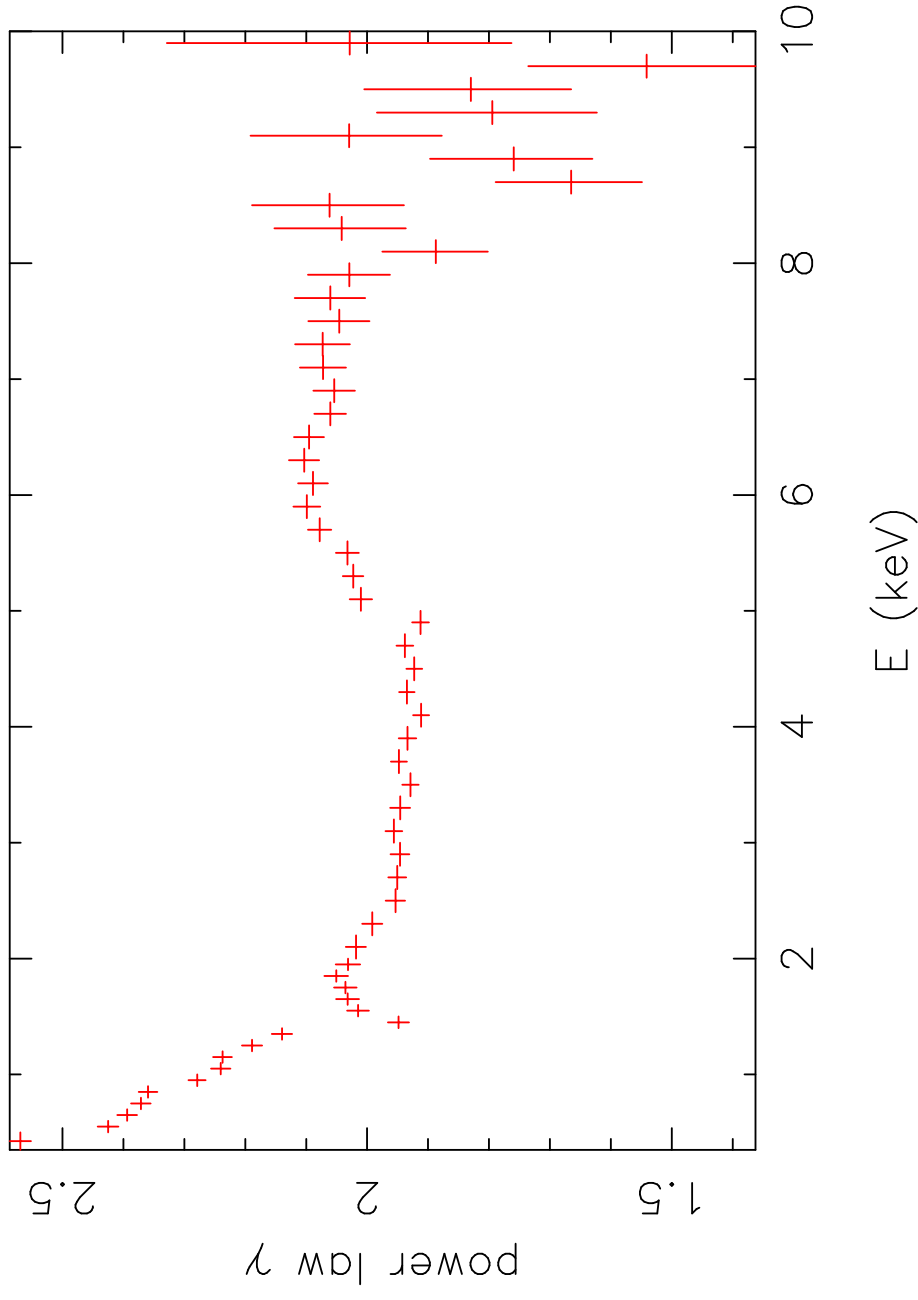
- construct an annular region, 2'' intervals out to 20'', then logarithmically-spaced out to 10'.
- clip the annuli at the edges of the S3 chip (allowing a margin for dither).
- mask the ACIS transfer streak with a narrow rectangle (8 pixels) streak from the main image.
- exclude detected sources.

Construct radial profiles from the narrow-band QE-corrected images: both Her X-1 and background data sets.

Fit the profiles for Her X-1 and the background simultaneously, using a constant background plus powerlaw model for the Her X-1 profile, and a constant background model for the background data set. The profiles were fit for $10'' \leq \theta \leq 590''$.

Powerlaw slope

The slope is steep at low energies, and ~ 2 for $E \sim 1.5 - 5$ keV. Above 5 keV, it gets somewhat steeper again. This is likely because the roughest mirror pair (MP1) rapidly loses effective area above 5 keV. For $E \gtrsim 8$ keV, the bins are too narrow, giving poor statistics.

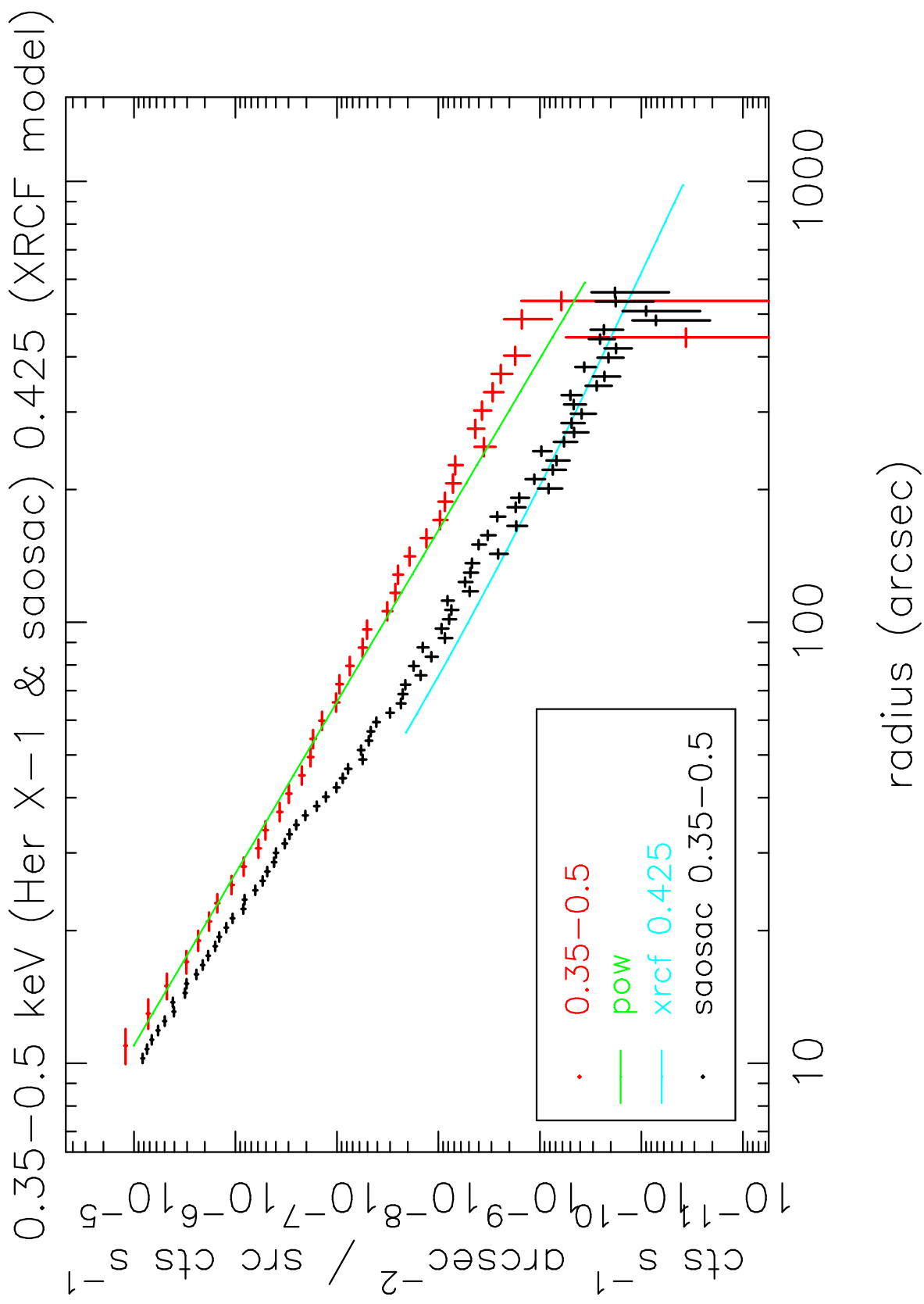


Normalization

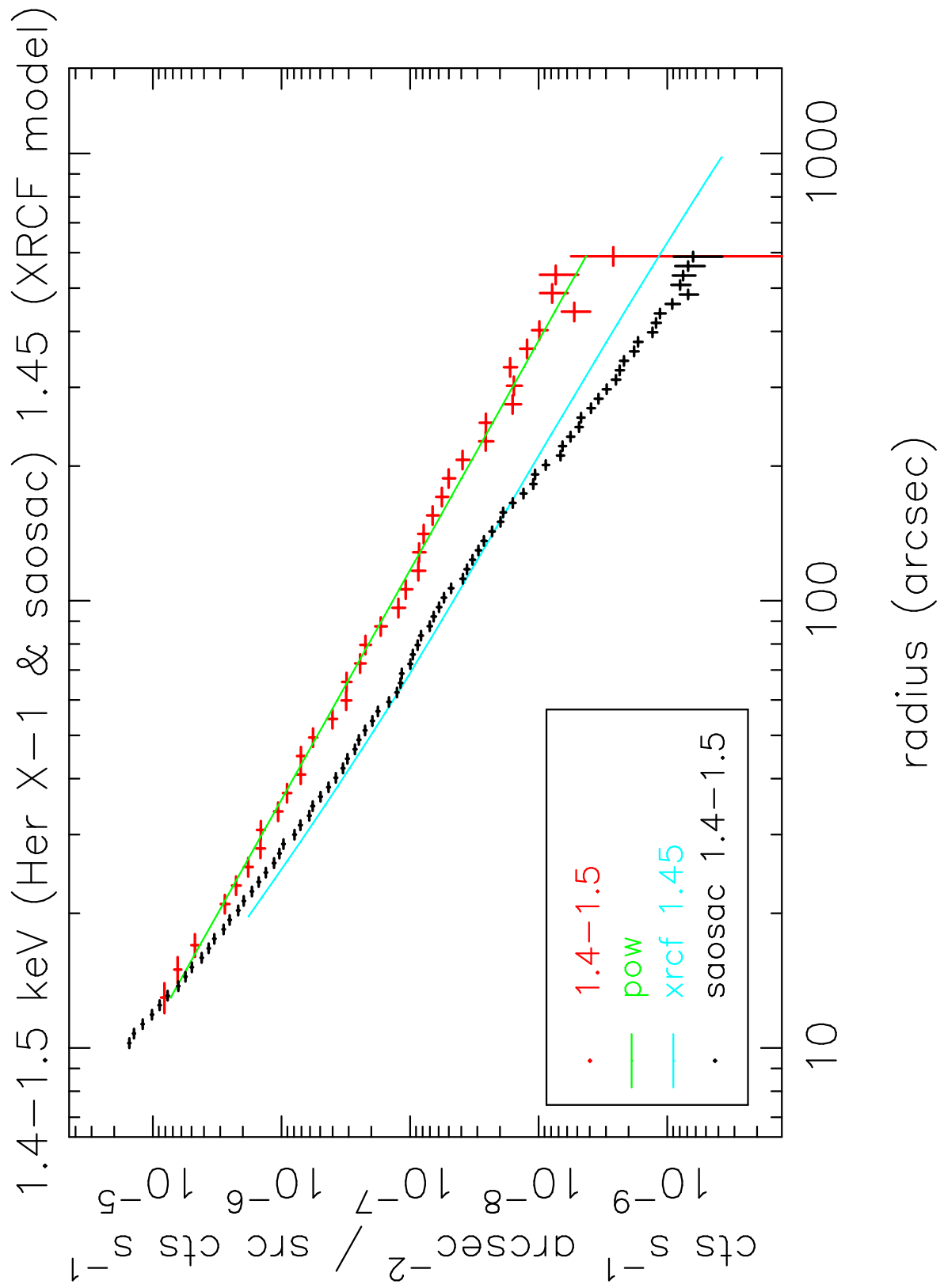
Ideally, normalize the profile by the count rate evaluated out to some fiducial radius encircling almost all of the scattered power. Because the source is heavily piled up, we do not have direct access to the count rate, and need to get at it indirectly.

- ACIS transfer streak: evaluate the count rate for a narrow rectangle centered on the transfer streak, but well away from the bright part of the halo. Scale count rate by: frame time / (streak length \times pixel transfer time) where
 - frame time is the ACIS frame time (3.1 s here)
 - length of the extracted rectangle in pixels = 609
 - pixel transfer time = 4×10^{-5} s/pixel

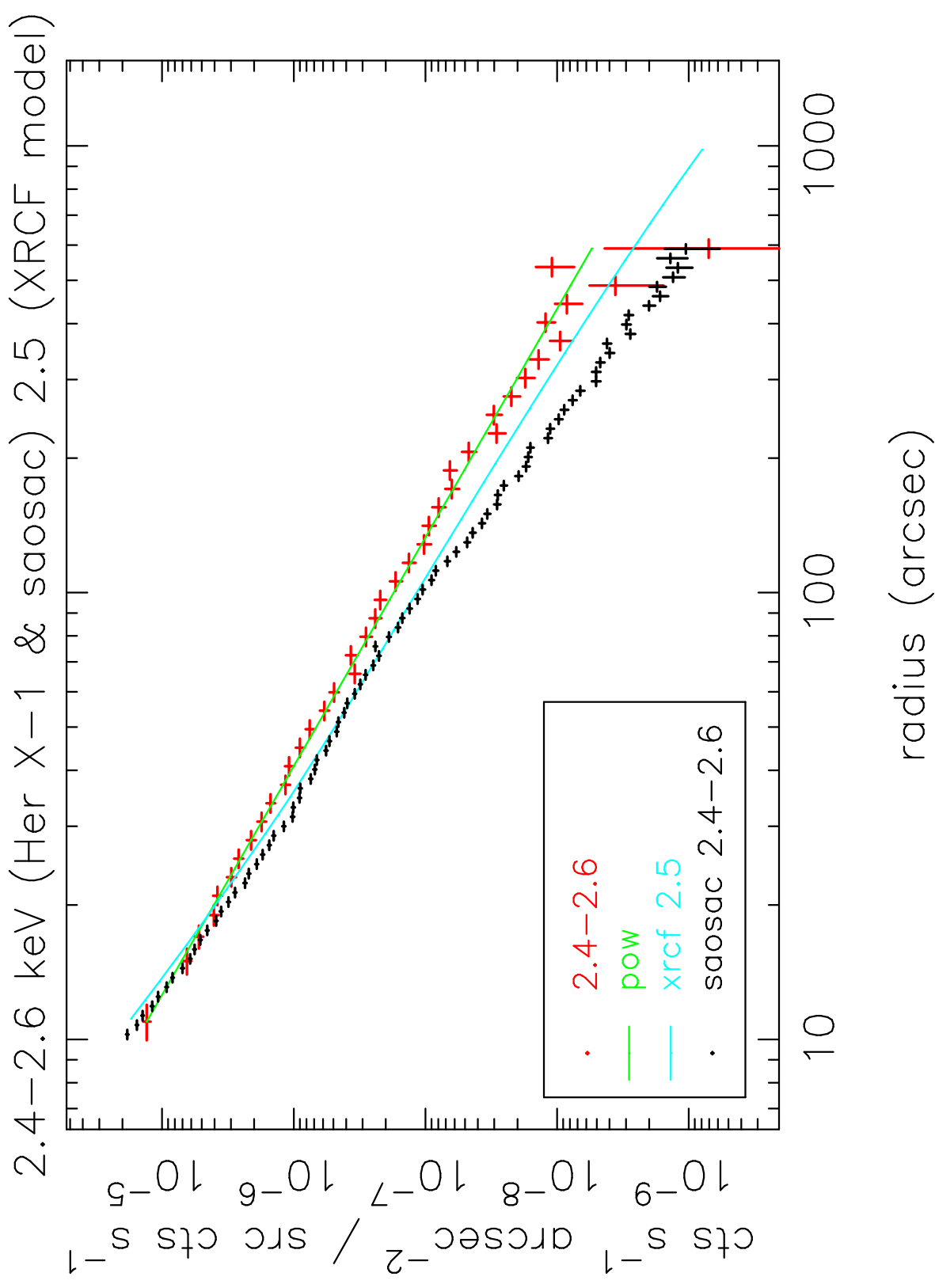
Profiles: 0.35-0.5 keV



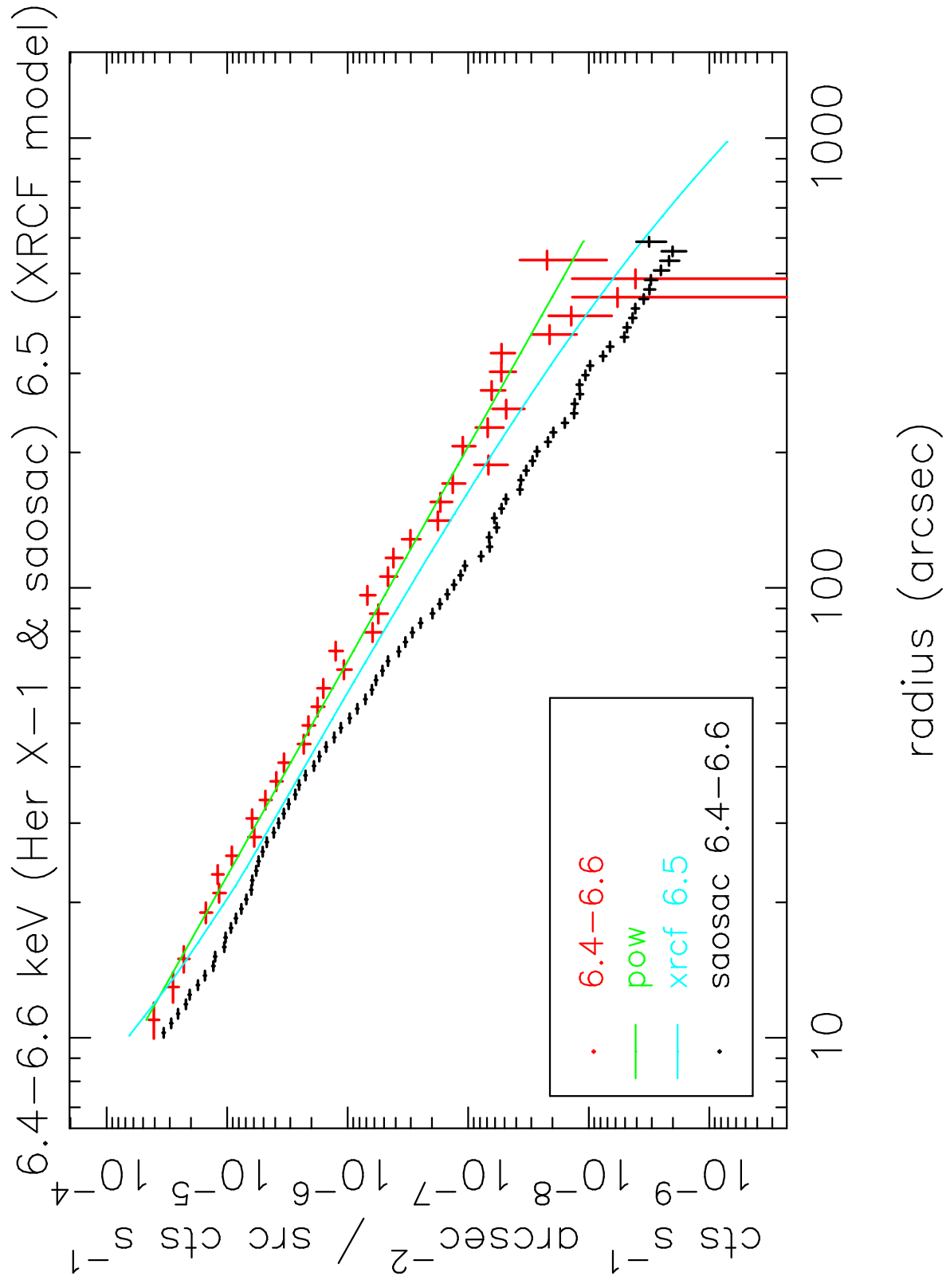
Profiles: 1.4-1.5 keV



Profiles: 2.4-2.6 keV



Profiles: 6.4-6.6 keV



Future Work

- summing over broader energy bins above 8 keV to improve S/N
- Reanalyze with VF-filtered source and background data
- CTI-correct and analyze the FI chip data
- improve limits from strut shadows
- ϕ -dependence of mirror scattering; expected to be small, but now it can be checked
- parameterized model

Summary

- The Her X-1 data allow significant progress in understanding the *Chandra* PSF wings.
- Narrow band radial profiles can be studied out to large radii; VF background filtering and adding in the I2, I3, and S2 data will help here.
- Reasonably detailed investigation of the angular (ϕ) distribution of the wings can be pursued.
- The model for the wings in the saosac raytrace model can significantly underestimate the wings at large radii (by a factor of ~ 5 , or more, depending on energy)
- Normalization issues remain to be investigated; particularly for energies below ~ 2 keV.